

Modeling Drying During Low-Speed Coating of Porous and Continuous Films

Richard A. Cairncross

University of Delaware, Mechanical Engineering Department, Newark, Delaware

Abstract

In low-speed dip coating (such as coating of sol-gel materials), airflow over the coating surface is uncontrolled and can be dominated by buoyancy-driven (natural) convection. Thus, there is a strong two-way coupling between the external gas flow and the drying of a thin film. To avoid solving a two-phase coupled transport problem (with drastically varying length scales), the thin-film transport is simplified into an elaborate 1D boundary condition on the gas-flow. Results of vapor transport and drying profiles are compared with and without the entrained film. The results show an increase in evaporation rate near the apparent "dryout line", due to increasing vapor diffusion parallel to the substrate. These predictions compare well with experimental results from imaging ellipsometry.

Introduction

In most industrial settings, drying is accomplished using high velocity impingement of hot air. The heat and mass transfer characteristics of these high velocity flowfields are fairly well correlated into heat and mass transfer coefficients. However, there are many situations where drying occurs under less controlled conditions with low airflow, such as low-speed dip coating, wicking of volatile solvents into porous media, and Marangoni drying. All of these situations are characterized by an airflow field which is subject to buoyancy-driven convection. For situations in which free convection occurs, there is a strong coupling between the flow of the gas and the heat or solvent vapor transport in the gas. In addition, when the buoyancy-driven flow arises from solvent evaporating from a coating, the flow field is a strongly coupled to liquid phase solvent transport in a thin film.

This paper focuses on drying during dip coating; i.e. withdrawal of a coating from a bath of coating solution without forced air convection. A goal of this paper is to explain experimental observations of Brinker et al. during dip coating of sol-gel coatings.¹ Because the substrate (on which the coating is deposited) is oriented vertically free convection occurs whenever there is a density mismatch between the solvent vapor and the air. For vapors heavier than air, such as ethanol, evaporation from a vertical substrate causes buoyancy-driven convection down the

surface of the substrate and enhances the evaporation rate. The buoyancy-driven flow in the gas can be adequately described by the Boussinesq approximation, because the overall density changes in the gas are small. The evaporation rate from the coating requires another equation describing the flux in a thin film. This paper treats the flux in the coating using a reduced-dimension formulation which converts the mass balance in the coating into a non-linear boundary condition on the gas phase solvent flux. Thus the full problem is reduced to a buoyancy-driven flow problem.

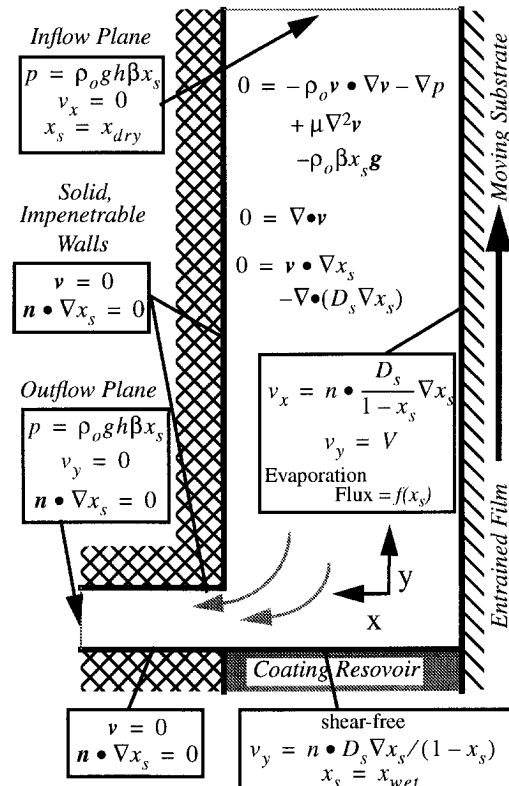


Figure 1. Schematic of dip-coating process with buoyancy-driven airflow over coating surface showing the computational problem with equations and boundary conditions labeled.

Theory

This paper presents a theory describing the coupling between solvent vapor transport in the drying gas and solvent liquid transport in a thin coating. Because the two transport processes occur on greatly different length scales, the

equations can be developed separately and later coupled to create a complete description. Figure 1 shows the basic geometry of a dip-coating process. As a film is withdrawn from a reservoir, solvent evaporates into the gas phase, and buoyancy-driven convection drives airflow over the coating.

This model in this paper incorporates a set of assumptions: 1) the coating surface is flat, 2) the coating reservoir is well mixed, 3) the inflow and outflow planes are fully developed and at hydrostatic pressure, 4) the solvent vapor is dilute 5) the airflow is laminar, and 6) the problem is isothermal. These assumptions set up the buoyancy-driven flow problem discussed in the next section. To simplify the analysis of the solvent transport in the entrained film, the model incorporates some additional assumptions: 1) the coating thickness is much less than the dimensions of the air-space, the length of the substrate, and the diffusion length scale, 2) the vapor at the surface of the coating is in equilibrium with the coating, 3) the solvent content at the inflow and outflow planes are known, and 4) the coating contains two components, a solid which moves at the velocity of the substrate and a solvent which can evaporate and diffuse relative to the substrate motion. The following sections discuss the application of these assumptions to develop the coupled drying model.

Free Convection

Within the gas-phase, the dominant physics are those of buoyancy-driven convection. The steady-state Navier-Stokes system of equations describes the momentum transport and mass conservation in this system. For buoyancy-driven flow, the equations are normally recast by subtracting a reference hydrostatic pressure from the hydrodynamic pressure and by assuming that the density variation only enters into the body force term (the so-called *Boussinesq approximation*)²:

$$-\rho_o \cdot \bar{\nabla} v - \bar{\nabla} \tilde{p} + \mu \bar{\nabla}^2 v - \rho_o \beta x_s g = 0 \quad (1)$$

$$\bar{\nabla} \cdot v = 0 \quad (2)$$

v is the mass-averaged velocity, ρ_o is the dry gas density, $\tilde{p} \approx p + \rho_o g y$ is the pressure in excess of hydrostatic pressure, and g is the gravitational body-force vector, $\beta = (\rho_o - \rho_s) / \rho_o$ is the volume expansion term for the gas, x_s is the volume-fraction of solvent vapor, ρ_s is the density of pure solvent vapor, and μ is the viscosity of the gas.

Solvent vapor transports through the domain by convection with the bulk gas and diffusion relative to the bulk convection. Assuming that the changes in gas density due to solvent vapor are small (<10% for saturated ethanol vapor at room temperature) the mass-averaged and volume-averaged velocities are equivalent, and diffusion-induced convection is negligible. This results in the standard form of the convection-diffusion equation for dilute species (using Fick's Law):

$$v \cdot \bar{\nabla} x_s - \bar{\nabla} \cdot (D_v \bar{\nabla} x_s) = 0 \quad (3)$$

D_v is the mutual diffusion coefficient of solvent vapor in air.

Equations (1), (2), and (3) along with the appropriate boundary conditions completely specify the buoyancy-driven convection problem. Along the solid wall, the gas velocity is zero and there is no penetration of solvent into the wall. At the top inlet to the domain, the solvent vapor concentration in air is known (assuming solvent is heavier than air) to be x_{dry} . At the bottom outlet, the solvent vapor transport is assumed to be pure convection (i.e. the gradient in concentration normal to the boundary is zero). The flow at both the inlet and outlet is assumed to be fully-developed and the pressure is assumed to be hydrostatic pressure at the given vapor concentration, $\tilde{p} \approx \rho_o \beta x_s g y$. Along the surface of the fluid reservoir a shear-free boundary condition is applied; thus the gas is allowed to flow tangentially along the fluid reservoir. Along the surface of the coating the tangential velocity is equal to the substrate velocity.

Along the surface of the fluid reservoir and the surface of the coating, the solvent vapor concentration is in equilibrium with the concentration of solvent in the coating solution and solvent evaporates into the gas phase. Thus, the normal component of the solvent vapor flux is equal to the volumetric evaporation rate of solvent vapor from the surface.³ If the evaporation rate of solvent is known (E in units of mass/area/time) then interfacial mass balances on solvent vapor and air in the gas phase give boundary conditions on the normal components of velocity and vapor diffusion at the boundary:

$$E = -n \cdot (v x_s \rho_s - n \cdot \rho D_s \bar{\nabla} x_s) \quad (4)$$

is a unit vector normal to the interface which is outward pointing from the gas phase. These equations assume that rate of shrinkage of the coating is small compared to the velocities in the gas phase. The evaporation rate E is determined by the film equations discussed in the next section.

Film Flow and Drying

The buoyancy-driven flow problem described in the preceding section is strongly coupled to the drying process of the coating as it is withdrawn from the bath. This coupling is caused by equilibrium between the solvent vapor concentration and the coating solution concentration; as the coating dries, the concentration falls and hence the solvent vapor concentration falls along the coating surface boundary. The two problems are strongly coupled because the drying process depends on the gas phase transport to determine the drying rate.

Assuming that the volume-change on mixing is small and that the coating does not contain porosity or void spaces, the shrinkage of a coating is equal to the volume of liquid solvent which evaporates. In this theory, the film is continuous because it contains no voids or inhomogeneities and compliant because it shrinks without stress (e.g. a polymer solution well above the glass transition temperature

of the polymer). Another publication in progress will extend these relationships for drying of unsaturated deformable porous media.^{4,5} In this paper the film is thin enough that solvent concentration is uniform through the coating thickness. Thus, a mass balance on a horizontal slice of the coating shows that the evaporation rate E from the surface of that slice must equal the difference in flux through the top and bottom surfaces of the slice:

$$E(y) = -\frac{d(hq)}{dy} \quad (5)$$

Here q is the solvent mass flux parallel to the coating in the direction parameterized by y , and h is the film thickness. In a continuous medium, the mass flux is split into convective and diffusive parts using Fick's Law:

$$q = VC_s - D_s \frac{dC_s}{dy} \quad (6)$$

V is the velocity at which the substrate and the coating are withdrawn from the bath, D_s is the mutual diffusion coefficient of solvent in the non-volatile species, and C_s is the solvent concentration. In general the mutual diffusion coefficient varies with solvent concentration; however the results in this paper use a constant diffusion coefficient. In addition, the solvent concentration in the coating liquid is also in equilibrium with the solvent vapor in the gas phase just above the coating surface: $x_s P = a(C_s) P_v^o$ with P the total pressure of the gas, $a(C_s)$ the activity of the solvent in solution, and P_v^o the vapor pressure of pure solvent. Although it is not necessary for this method, the results in this paper assume that the equilibrium relationship follows Raoult's law: $x_s P = P_v^o C_s / \rho_l$. ρ_l is the density of pure liquid solvent.

Because there is no volume-change on mixing, the coating thickness is a sum of a thickness due to the solvent, $h C_s / \rho_l$ and a thickness due to the non-volatile component, $h(1 - C_s / \rho_l)$. Because the non-volatile component does not evaporate its thickness remains constant, and the coating thickness is a function of the solvent concentration in the coating:

$$h = h_o \frac{(1 - C_s^o / \rho_l)}{(1 - C_s / \rho_l)} \quad (7)$$

h_o and C_s^o are the initial coating thickness and solvent concentration, respectively. Using the equilibrium equation, the thickness is a function of solvent vapor concentration.

Combining equations (5), (6), and (7) and Raoult's law gives a balance equation for the evaporation rate in terms of the gas-phase solvent vapor concentration:

$$E(y) = -h_o \rho_l \left(l - x_s^o \frac{P}{P_v^o} \right) \left(\frac{P}{P_v^o} \right) \frac{d}{dy} \left(\frac{v x_s - D_s \frac{dx_s}{dy}}{1 - x_s \frac{P}{P_v^o}} \right) \quad (8)$$

Here x_s^o is the solvent vapor volume fraction that would be in equilibrium with the initial coating solution. Roughly, the coefficient on the right-hand-side is the mass of solvent which is available for evaporation and the term inside the differential is the driving force for evaporation. Thus, the mass balance on a thin film gives an equation for the evaporation rate in terms of the solvent vapor concentration, the gradient of the solvent vapor concentration, and a set of known constants. This equation becomes a nonlinear boundary condition on the solvent flux in the gas-phase flow through equation (4).

Numerical Solution of the Equations

Numerical methods for solving the Navier-Stokes equation system with a Boussinesq approximation for buoyancy-driven convection are well established in the literature. The computations in this paper exhibit Reynolds numbers between 0.5 and 100 justifying the laminar flow assumptions. Galerkin's method with finite-element basis functions (GFEM) is a well proven method for solving incompressible fluid-mechanics problems. The results in this paper were calculated using GOMA, a general-purpose computational fluid-dynamics from Sandia National Labs.⁶

Solution by GFEM proceeds by interpolating the variable x_s by a basis set using the weighting functions a basis functions. This produces a non-linear system of equations with an equal number of equations and unknowns, which is solved by Newton's method and a sparse direct solver. The integrals are evaluated by using 3-point Gaussian quadrature in each direction. The weighting and basis functions for the momentum equations and solvent transport equations are 9-node biquadratic functions on each element and continuous between elements, and the weighting and basis functions for the continuity equations are bilinear on each element but discontinuous between elements. The results in this paper were computed on a Sun SparcStation10. The discretization was unstructured and tested for convergence by refinement.

Results

The theory discussed above describes buoyancy-driven flow in the air cavity surrounding a dip-coater. For the results presented below, the solvent is ethanol and the drying gas is air. The coating entering the domain contains 95% solvent by volume. Figure 2 compares the predictions with and without an entrained coating. In the case of no coating, the evaporation rate is zero along the substrate, and the vapor concentration profiles are nearly horizontal. This result exhibits diffusion of solvent vapor vertically from the bath

against a flow of gas downward through the domain. The gas flows downward because ethanol vapor is heavier than air (Molecular weight of Ethanol is 46 while molecular weight of Air is 29). Also the streamlines for the results without an entrained coating are smooth as the vapor passes through the domain.

An entrained film moving with the substrate draws solvent upward along the coating boundary before it evaporates; thus the entrained film acts like a source of solvent vapor. This results in higher solvent vapor concentrations along the coating boundary and a horizontal gradient in solvent vapor concentration. The horizontal concentration gradient causes faster air convection near the coating and diverts the streamlines towards the substrate.

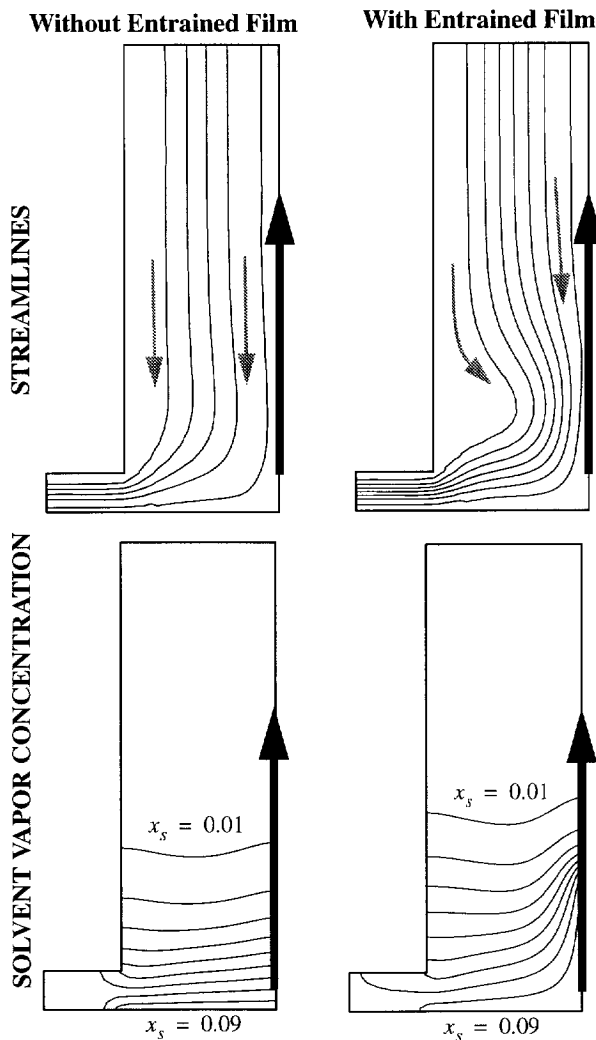


Figure 2. Comparison of predictions for flow streamlines (contour intervals = 0.05 cm^{2/s}), solvent vapor concentration (contour intervals = 0.01 volume fraction) with no entrained film and a continuous (polymeric) film, (5 mm initial film thickness, 95% initial solvent content, and 1 mm/s substrate speed).

The thickness profile (Figure 3) shows an increasing rate of thinning as the film approaches a “dryout” line (at $y \approx 1.7$). Such an increasing drying rate has been observed experimentally by Hurd using imaging ellipsometry^{1,7}. By analogy of the vapor diffusion problem to a electrostatic potential problem, Hurd showed that the evaporation rate of a pure solvent film should be inversely proportional to the square-root of the distance from the dry-out line and that the thickness should be proportional to the square-root of the distance from the dry-out line:

$$h(\tilde{y}) = c\tilde{y}^{1/2}, E(\tilde{y}) = c\rho_l V\tilde{y}^{-1/2} \tag{9}$$

$\tilde{y} = y_{dryout} - y$ is the distance from the dryout line, and c is a constant related to the diffusivity of solvent vapor and the geometry. Equation (9) exhibits an integrable singularity in the evaporation rate at the dryout line. The drying rate increases because at the dryout line, more dry air is accessible for diffusion (the vapor concentration contours become tightly clustered) than far below the dryout line (the vapor concentration contours are nearly vertical and well spaced). The predictions in this paper differ from Hurd’s theory because the air is not stagnant and the coating is not pure solvent. Nevertheless, the drying profile fits very well with Hurd’s theory over a distance of about 1 cm below the dryout line (as in Figure 3).

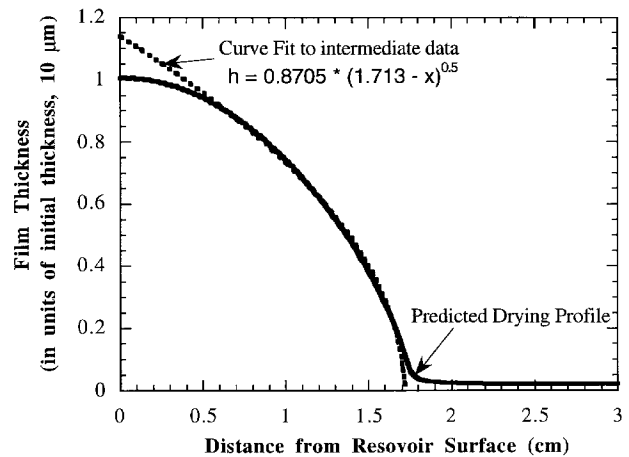


Figure 3: Drying of a thick (10 mm) continuous film with low initial solids content (2%) with a curve fit to Hurd’s parabolic drying profile

Conclusions

The dryout line in these predictions corresponds to an inflection point in the drying rate where the solvent vapor concentration begins to drop sharply. As the solvent vapor concentration drops, so does the drying rate and the thickness profile asymptotically approaches the dry film thickness. A consequence of the sharp increase in evaporation rate near the dryout line is that the effective mass transfer coefficient is

not constant along the film. Thus the common assumption of a constant mass transfer coefficient is inappropriate for these problems because the transport in the gas phase controls the drying rate. Similar results are also predicted for drying of deformable porous media.^{4,5}

Acknowledgments

This work was performed under a contract from Sandia National Laboratories which is supported by the United States Department of Energy under contract DE-AC-4-76-DP85000. The author would also like to thank Jeff Brinker, Randy Schunk, and Phil Sackinger for many fruitful discussions that lead to the results in this paper.

References

1. C.J. Brinker, A.J. Hurd, P.R. Schunk, G.C. Frey, and C.S. Ashley, "Review of Sol-Gel Thin Film Formation", *J. Non-Crystalline Solids*, **147 & 148** (1992) 424-436.
2. R.B. Bird, W.E. Stewart, and E.N. Lightfoot, "Transport Phenomena", Wiley (1960) §3.5
3. P. R. Schunk, and R.R. Rao, Finite Element Analysis of Multicomponent Two-Phase Flows with Interphase Mass and Momentum Transport, *Int. J. for Numerical Methods in Fluids*, **18** (1994) 821-842
4. R.A. Cairncross, P.R. Schunk, K.S. Chen, J. Samuel, S. Prakash, C.J. Brinker, and A.J. Hurd, "Drying in Deformable Partially Saturated Porous Media: Sol-Gel Coatings", *Sandia Report SAND96-2149* (1996).
5. R.A. Cairncross, P.R. Schunk, K.S. Chen, J. Samuel, S.S. Prakash, C.J. Brinker, and A.J. Hurd, "Pore Evolution and Solvent Transport During Drying of Gelled Sol-To-Gel Coatings: Predicting Springback", *Drying '96*, A.S. Majumdar, ed. (1996).
6. P.R. Schunk, P.A. Sackinger, R.R. Rao, K.S. Chen, and R.A. Cairncross, "GOMA- A Full-Newton Finite Element Program for Free and Moving Boundary Problems with Coupled Fluid/Solid Momentum, Energy, Mass, and Chemical Species Transport: User's Guide", *Sandia Report SAND95-2937* (1996).
7. A.J. Hurd and C.J. Brinker, Sol-Gel Film Formation by Dip Coating, presented at the AICHE Spring National Meeting, Orlando, FL (1990)